#6359

Building and Environment, Vol. 27, No. 4, pp. 433–445, 1992.
Printed in Great Britain.

0360–1323/92 $5.00 + 0.00
© 1992 Pergamon Press Ltd.

Physical and Numerical Modelling of a Solar Chimney-based Ventilation System for Buildings

G. S. BAROZZI*
M. S. E. IMBABI†‖
E. NOBILE*
A. C. M. SOUSA‡

This paper describes an experimental and numerical study to analyse the thermal performance of a bio-climatic building prototype in Nigeria. The roof performs as a solar chimney, generating an air flow through the living space of the building to provide cooling. Experimental tests on a 1:12 small-scale model of the prototype are outlined, and the results, both qualitative and quantitative, are used to validate a two-dimensional flow simulation model, in which the steady state conservation equations of mass, momentum and thermal energy are solved using a finite volume formulation.

The experimental and numerical results, expressed in terms of temperature and velocity fields, for two different window geometries are critically evaluated and compared with good agreement.

NOMENCLATURE

- g Gravity constant, m s^{-2}
- H Total height of experimental model, m
- P Pressure, Pa
- T Temperature, K
- U Horizontal velocity component, m s^{-1}
- V Vertical velocity component, m s^{-1}
- X Horizontal coordinate, m
- Y Vertical coordinate, m

Greek symbols

- α Thermal diffusivity, m^2 s^{-1}
- β Volumetric coefficient of expansion, K^{-1}
- ν Kinematic viscosity, m^2 s^{-1}
- ρ Density, kg m^{-3}.

INTRODUCTION

INDOOR thermal comfort is a function of temperature, air flow, relative humidity, and radiation [1, 2], and methods of controlling, or modifying these parameters, must be taken into consideration throughout the useful life of a building. Today's technology can be used to provide any desired thermal state, irrespective of building form or location, but the economic penalty is high. The limitations of conventional energy sources, in terms of cost and availability, and an increased awareness of environmental issues, have led to renewed interest in passive building design.

Passive solar heating, in which part or all of the building is a solar collector, has been widely examined [3, 4], passive solar cooling, however, remains largely unexplored. One interesting application of this technology, particularly appropriate for hot-humid climates, is to interior ventilation by using a solar chimney to induce buoyancy-driven flow. Such a ventilation system is examined qualitatively and quantitatively in the present work.

Motivation, objectives, and expected benefits

The need for passive cooling strategies is greatest in developing countries, where hot annual temperatures are predominant. Constrained by extreme environmental conditions, poor building technology, and limited financial resources, these countries have had little opportunity to establish good standards of thermal comfort in buildings. In many instances, indigenous architecture has been superseded by imported *modern* building design. Compounded by the cost of foreign-made materials and components, the increased fuel consumption required to keep these buildings cool has invariably contributed to financial ruin.

A collective effort is therefore required to develop new passive building technologies for the Third World. The use of low-cost, readily available building materials, and simple construction methods should be encouraged, and passive means of cooling the building must be utilized. New predictive tools, capable of dealing with the latter aspect, are urgently needed.

Following the latter approach, an experimental passive solar building [5] was recently completed in Ife (Nigeria). A solar chimney roof, to promote air flow within the

* Istituto di Fisica Tecnica, Università di Trieste, 34127 Trieste, Italy.
† Department of Engineering, King's College, Aberdeen AB9 2UE, U.K.
‡ Department of Mechanical Engineering, University of New Brunswick, N.B. E3B 5A3, Canada.
‖ Previously Visiting Fellow at International Centre for Theoretical Physics, Trieste, Italy.

building envelope, is a novel feature of the Nigerian prototype. Apart from reducing thermal stratification, it is anticipated that the solar chimney will move a sufficient quantity of air inside the building to cool the occupants. Well established methods for passive cooling, such as nocturnal and evaporative cooling [6], are of little use in the hot-humid climate of Nigeria, where temperatures over 35°C and relative humidities over 80% are not unusual.

A solar chimney generates air movement by buoyancy forces, in which hot air rises and exits from the top of the chimney, drawing cooler air through the building core in a continuous cycle. For the anticipated operating conditions of the full-scale prototype, the flow through the chimney may reach the transitional and/or turbulent regimes. This aspect, associated with the complexity of the building's geometry, demands considerable physical insight into the problem, in order that appropriate strategies are developed. To carry out the evaluation of the solar chimney performance, a 1:12 small-scale model of the Nigerian prototype was built, and tested under simulated climatic conditions. In parallel with this, a two-dimensional Computational Fluid Dynamics (CFD) simulation of the small-scale model was performed. The objectives of the present work are to study the convection mechanism, and as full-scale results become available, to improve our knowledge of modelling techniques for buildings in general.

Planning for full scale experimental tests is being carried out in Nigeria, but before acquisition, processing and analysis of the data are effected, as may be expected, a considerable amount of time will have elapsed. In the interim, experimental results from the small-scale model are used to validate the numerical procedure, which, in due course, will be used to predict full-scale performance.

Scale model review

Scale models of buildings, to predict thermal effects, have been in evidence for a number of years. In addition to their relatively low cost—when compared to full-scale models—they sometimes offer the only viable means for studying certain aspects of the building design under controlled laboratory conditions. The use of scale models for building energy simulation has, however, been vigorously debated since the early tentative applications as referred in [7].

Building energy is primarily governed by three mechanisms of heat transfer—conduction, radiation, and convection, this being most difficult to model at a reduced scale. Perfect similitude for buoyancy-driven flows, which is of particular interest in the present case, requires that the dimensionless governing equations remain identical, which implies that at least two dimensionless numbers, the Prandtl (Pr) and Grashof (Gr) numbers,

$$Pr = \frac{\nu}{\alpha}; \quad Gr = \frac{\beta g L^3 (T_1 - T_0)}{\nu^2}$$

have the same value for the model and the building.

From the above definitions, it is clear that strict similitude is not possible when the same gas, i.e., same Pr, is used in both the model and prototype. This is due to the presence of L^3 in the Grashof number, Gr. On the basis of this argument, the validity of small-scale building models has been questioned, and it has been suggested that only full-scale (1:1) models should be used [8].

Such a constraint is clearly not practical for buildings! One alternative may be to work with higher temperature differences, to compensate for the reduction in L^3. Thus, for a half-scale model, the temperature difference must increase by a factor of 8. Air properties, however, change with temperature, and it should be noted that long-wave radiation is proportional to T^4! Another alternative is to use a different fluid medium in the scale model. Various gases and gas mixtures have been suggested [9, 10], but this approach tends to affect heat and fluid flow characteristics. Moreover, the method is absolutely impractical for the modelling of *open* systems, such as ventilated buildings. Others have postulated that for turbulent forced convection, even if dynamic similitude is not maintained, kinematic similitude (i.e., similar velocity profiles) can occur [7]. It has been suggested that the same should apply to buoyancy dominated flow regimes above a critical value of the Rayleigh number ($Ra = Pr \times Gr$). Attempts to validate this hypothesis for enclosed systems [7, 11], however, are not entirely conclusive. The problem of modelling the thermal behaviour of real buildings is much more complex, since they are open to, and interact freely with the outside world. External factors, such as temperature, wind speed, and solar radiation can influence the thermal response of the building, and should be considered accordingly.

Due to the constraints and difficulties associated with full similitude, and depending on the information that a scale model is expected to provide, it is postulated that partial similitude, in which geometry and boundary conditions are properly scaled, can produce meaningful results.

In a previous study [12], dimensional analysis was used to derive the thermal properties for a 1:7 scale model building and HVAC plant, with the objective of rapidly testing and demonstrating the performance of various automatic HVAC control systems. Good agreement with recent computer simulation results was obtained [13], and similar argument may apply to the buoyancy induced ventilation (solar chimney) system under consideration.

It is expected that the information obtained from a small-scale model of the Nigerian prototype can be used to give a good design guideline by identifying the main features of the flow pattern, such as regions of stagnation, flow entrainment, and flow velocities. In addition, the small-scale model data will be used to test and to benchmark the numerical model, which, once validated, will be a state-of-the-art predictive tool.

Numerical modelling—a brief overview

Computational Fluid Dynamics (CFD) applied to the analysis of energy and/or safety in buildings, has grown in importance in recent years. Early trials indicate a wide range of opportunities for the use of CFD in building analysis. However, there are some reservations on the validity of commercial CFD codes for building energy simulation. They arise not only from the *complexity* of CFD programs, but also from difficulties associated with the proper definition of boundary conditions [14].

In [15] two-dimensional steady-state calculations of

velocity and temperature fields are presented for a room with a ventilation system. The difference between predictions and experimental observations for maximum velocity and for maximum temperature, was less than 4% and 5%, respectively. Previous work [16], had given further evidence of the versatility and potential of the numerical technique used by computing relative humidity in air conditioned rooms and cold stores.

In [17], basic Finite Volume techniques are reviewed for simulation of air movement and convective heat transfer within buildings. Several successful 2D and 3D applications were reported, and it is strongly emphasized that CFD codes cannot be used as *black boxes*, and that proper engineering judgement must be exercised in applying and in interpreting the output from CFD simulations.

Predictions of room ventilation quality were reported in [18, 19]. In both cases 3D steady-state flow fields were computed by means of standard two-equation $(k-\varepsilon)$ turbulence models. For both, the comparison between predictions and experimental data was reasonably good, and within the limits of the experimental accuracy, and the uncertainties in establishing the boundary conditions.

An interesting evaluation of ventilation and temperature efficiency in a room is given in [20], for four different kinds of ventilation systems. The primary goal of this work was to study airflow, contaminant concentration distribution and the temperature field, in order to improve energy efficiency and air quality. Time-dependent calculations were performed using a commercial CFD package, and good agreement between measurements and predictions was obtained. These field calculations are computationally demanding; even so, the use of CFD simulation to obtain more precise cooling load predictions is advocated by the authors. In a recent work [21], CFD was used to quantitatively compare the energy efficiency, the draught distribution and indoor air quality of three different heating systems in an office room.

Finally, it is worth noting the growing interest in *fire simulation* using CFD. As an example, in [22] the 2D CFD modelling of combustion products is described for a room fire. The computer model validation was done against the experimental measurements obtained in a shopping-mall test facility. Reasonable agreement is reported, despite some considerable uncertainties associated with the turbulence model employed and 3D effects, which were not accounted for in the model.

THE PROTOTYPE AND THE MODEL

An experimental prototype bioclimatic building was recently completed in Ife, Nigeria (7.5°N, 4.6°E). It consists of a single chamber, roughly $5.5 \times 3.5 \times 3.0$ m^3 in size ($L \times W \times H$), with a corrugated metal roof and fibreboard ceiling. The roof is provided with the novel feature of an integral solar chimney to promote ventilation and cooling. Walls are made of light, removable wooden panels, allowing different window arrangements to be examined. The building may be classified as a low cost/energy design, appropriate for Nigerian conditions. Building form and construction details are summarized in Fig. 1.

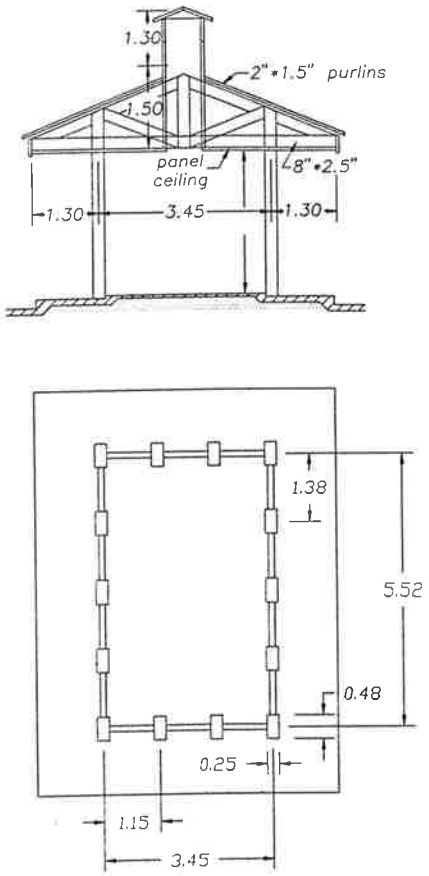

Fig. 1. Nigerian prototype building.

Based on dimensional analysis, the physical characteristics of the prototype were translated to design specifications for a small-scale model building [23], and to simplify the problem, only those parameters expected to have the greatest effect on the environmental response of the building (including temperature and solar radiation) were considered. A 1 : 12 scale replica of the prototype was built, and, where possible, the original materials of construction were employed. This has led to a considerable simplification since scaling of densities and specific heat capacities was not required. Figure 2 depicts the model and its main dimensions, and in addition details of the two window configurations are given. It can be observed that, for both geometries, the window size is the same, the only difference being their relative position above ground level.

THE EXPERIMENT

Introduction

Due to the exploratory nature of the present study, this was restricted to the steady-state response of the model, and climatic factors were limited to the ambient outdoor temperature and solar radiation with the latter limited to vertical incidence, to ensure maximum irradiation and symmetry. Relative humidity was assumed to be constant, as is usually the case in hot-humid climates. In addition, the combination of no wind and overhead sun was taken as the scenario posing the

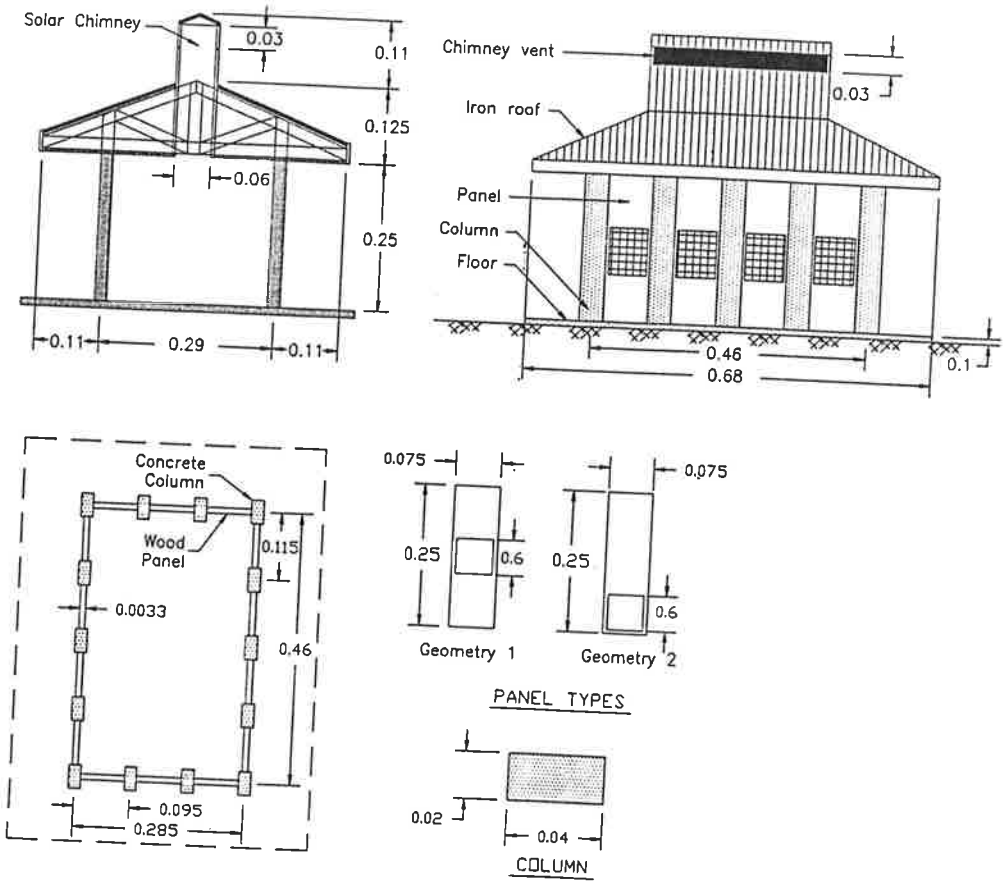

Fig. 2. Model building details and dimensions.

highest demand upon the ventilation system. In reality, this choice is close to the actual conditions since in the Ife region the prevailing wind speeds are weak (less than 6 km h^{-1}).

The physical model was designed with the objective of providing approximately equal prototype-to-model ratios for time scale and length scale. This has the combined effect of simplifying the experimental setup, and shortening the duration of tests. Since 2 h of real time represented 1 day for the model, and since diurnal temperature changes in Nigeria are small, the need to create a simulated outdoor environment was eliminated. A sealed laboratory chamber, with blanked windows, was used to simulate idealized weather conditions over 24 h of model time, and the reliability and repeatability of the data were assessed by conducting several series of tests over an extended period of time.

Instrumentation and experimental procedure

A solar simulator was used to heat the roof of the model, and the approach to steady-state was monitored with a PC data-acquisition system. Once steady-state behaviour was observed, converted sensor readings were written to a data file, for future evaluation. Measurements of temperature and air velocity were confined to a reference vertical plane, as shown in Fig. 3, for future comparison with the numerical results. Air velocity measurements were complemented with smoke-trace visualization of the flow field within the model building.

Solar simulator. The theoretical peak global solar irradiation at Ife, Nigeria, was estimated at 900 W m^{-2}. Due to scaling effects, this translated to 815 W m^{-2} for the model. Four Osram Ultra-Vitalux lamps, individually rated at 300 W, were used to construct a simple solar simulator. At 0.5 m above the horizontal, these lamps

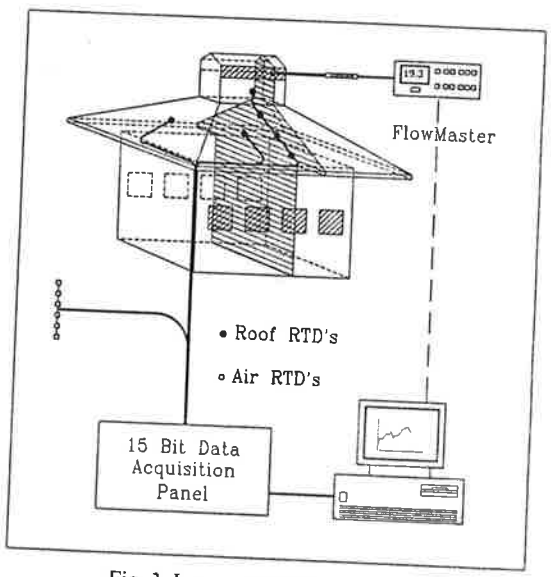

Fig. 3. Instrumentation schematic.

were designed to give an average of 800 W m^{-2}, spread over an area of 0.3×0.3 m. Lack of detailed meteorological and experimental data from Nigeria, and the dictates of steady-state testing, however, preclude the need for a more elaborate design. The solar simulator and model building are schematically presented in Fig. 4.

Data acquisition system. A general purpose data-acquisition system was developed to assist the experimental tests. An IBM AT-compatible microcomputer was fitted with a Burr Brown DMA series 20000 data acquisition carrier card and input/output expansion peripherals. A computer program was written and compiled for the system, supporting up to 24 analogue inputs, 15 bit A/D conversion accuracy, programmable gain for individual channels, text and graphics, and calibrated, averaged output. The system speed was just under 1800 scans s^{-1}.

Temperature measurement. Twelve miniature Heraeus Platinum Resistance Thermodetectors (PRT) were calibated for temperature measurement, and connected to the data-acquisition system. Calibration was performed using a thermostatically controlled bath and high precision (± 0.01°C) reference thermometer. To ensure the highest possible accuracy, all PRTs were energized using a stabilized power source, linearized, and balanced to eliminate cable effects. The overall accuracy of temperature measurements was estimated to be better than 0.2°C.

Six surface mounting type PRTs were permanently attached to the underside of the metal roof and solar chimney. This was done to provide experimental temperature data for comparison with predictions obtained from CFD analysis, and to correct for variations caused by drift in test conditions. The remaining PRTs were of the free mounting type, and were used to perform sequential measurements at various locations within the model building.

Velocity measurement. Air flow velocities were determined at the solar chimney outlet, using Dantec 54N50 Low Velocity Analyser, a temperature compensated anemometer. The hot film probe used is a 3 mm glass sphere with a deposited nickel thin film, which gives an approximate spatial resolution of ± 3 mm. No other meaningful velocity measurements were possible, since the very low velocity values, less than 5 cm s^{-1}, at other flow sections, produced unacceptable measurement uncertainties. The accuracy of air velocity measurements was estimated as $\pm 20\%$ in the 5–50 cm s^{-1} range.

Flow visualization. Perspex wall panels were fitted at the reference section, and across one end of the building, to provide a clear view of the interior. A system was built to generate dense white smoke which, when sufficiently cooled down, was gently injected through a slotted nozzle near the reference section inlet (window). Smoke trails were enhanced, using a laser sheet, and recorded on video tape and 35 mm slide film. Images of the flow pattern through the interior of the building, and inside the roof/ceiling cavity, were then compared to numerical predictions. The process was repeated for both model geometries.

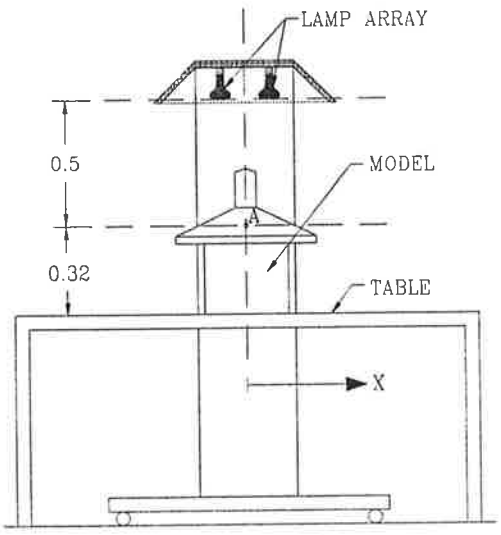

Fig. 4. Solar simulator.

MATHEMATICAL MODEL

The full description of the flow and heat transfer for the model may require a 3D formulation, eventually taking into account transitional and/or turbulent phenomena, and combined convection/conduction and radiation effects. This is a formidable task, even considering that for the problem at hand, it is possible to simplify the geometry by taking into account the symmetries of the model. Extensive computational resources would be required, which, at this stage, cannot be justified. In addition, the formulation may require a turbulence closure, such as two-equation $k-\varepsilon$ [24], or the more sophisticated Reynolds Stress Model (RSM) or Algebraic Stress Model (ASM) [25]. None of these closures, however, guarantees accuracy, since they are still under development and testing, particularly when applied to buoyancy-driven flows [26]. Furthermore the appropriate choice of the boundary conditions is still open to debate, and consequently, as a first step, it was decided to conduct the numerical analysis for a simple model, but general enough to allow the implementation of future extensions and modifications. Its main assumptions can be summarized as follows:

- The problem is two-dimensional.
- Radiation, inside the building, is negligible.
- Flow is steady and laminar.

The 2D model corresponds geometrically to a transversal section of the model across one of the windows, as shown in Fig. 3, for both geometries #1 and #2.

Governing equations

The governing equations are written for a steady, two-dimensional buoyancy driven flow under the Boussinesq approximation, i.e. density variation is only taken into account in its contribution to the body force. The length scale is chosen as the height, H, of the experimental model, with T_0 as the ambient (reference) temperature and T_1 the highest temperature, measured off the metal roof in the model.

The non dimensional variables are defined as follows:

$$x=\frac{X}{H};\quad y=\frac{Y}{H};\quad u=\frac{UH}{\alpha}$$

$$v=\frac{VH}{\alpha};\quad p=\frac{PH^2}{\rho\alpha v};\quad t=\frac{T-T_0}{T_i-T_0}.$$

The dimensionless numbers are Prandtl number (Pr), Grashof number (Gr) and Rayleigh number (Ra).

The following equations respectively describe conservation of mass, momentum components, and energy in Cartesian coordinates:

$$\frac{\partial u}{\partial x}+\frac{\partial v}{\partial y}=0 \tag{1}$$

$$\frac{1}{Pr}\left(u\frac{\partial u}{\partial x}+v\frac{\partial u}{\partial y}\right)=-\frac{\partial p}{\partial x}+\left[\frac{\partial^2 u}{\partial x^2}+\frac{\partial^2 u}{\partial y^2}\right] \tag{2}$$

$$\frac{1}{Pr}\left(u\frac{\partial v}{\partial x}+v\frac{\partial v}{\partial y}\right)=-\frac{\partial p}{\partial y}+\left[\frac{\partial^2 v}{\partial x^2}+\frac{\partial^2 v}{\partial y^2}\right]+Ra\,t \tag{3}$$

$$u\frac{\partial t}{\partial x}+v\frac{\partial t}{\partial y}=\left[\frac{\partial^2 t}{\partial x^2}+\frac{\partial^2 t}{\partial y^2}\right]. \tag{4}$$

The two geometries studied are depicted in Fig. 5(a) and (b). Due to symmetry, only half section was modelled, a simplification which would not have been possible for non-symmetric insolation. The boundary A–B, to minimize its influence upon the flow, is set at some distance upstream of the inlet aperture, and with reference to Fig. 5(a) and (b), the following boundary conditions were used:

1. Velocity.

$$A-B:\frac{\partial v}{\partial x}=0 \qquad B-C: \quad u=v=0$$

$$C-D:u=0;\frac{\partial v}{\partial x}=0 \qquad D-E: \quad u=v=0$$

$$E-F:\frac{\partial v}{\partial x}=0 \qquad F-G,G-A: \quad u=v=0. \tag{5}$$

The velocity components are also set to zero at all internal walls.

2. Pressure. The value of pressure, rather than velocity components, were specified at inlets and outlets as follows:

$$A-B:p=0 \quad E-F:p=0. \tag{6}$$

3. Temperature.

$$A-B:t=0 \qquad B-C:t=t_{ground}$$

$$C-D:\frac{\partial t}{\partial x}=0 \qquad D-E:t=1$$

$$E-F:\begin{cases}\dfrac{\partial t}{\partial x}=0 & \text{if } u<0\\ t=0 & \text{if } u\geq 0\end{cases} \qquad F-G:t=t_{roof}$$

$$G-A:\frac{\partial t}{\partial x}=0. \tag{7}$$

The computational temperature boundary condition at the roof, t_{roof}, and at the ground in the interior of the model, t_{ground}, were set at the same values of the experimental tests. While these boundary conditions do not pose any particular problem, in the sense that they are derived from measurements and geometric considerations, the flow boundary conditions at inlet and outlet are somewhat more difficult. In fact, in the open literature, there is not much agreement about what boundary conditions can be used for buoyancy-driven flows with openings [22, 27]. Choosing an appropriately *larger* domain would reduce the possible sources of error, but again this increases the computational cost. Also, the common practice of fixing the value of the pressure at *inlets* to that of the ambient, and subtract the *local kinetic energy head*, is of doubtful validity, since it is true only for one-dimensional, non-viscous flow problems. So, as a compromise, the following simplifying assumptions for the boundary conditions were made:

- The kinetic energy head is neglected at the inlet boundary A–B.

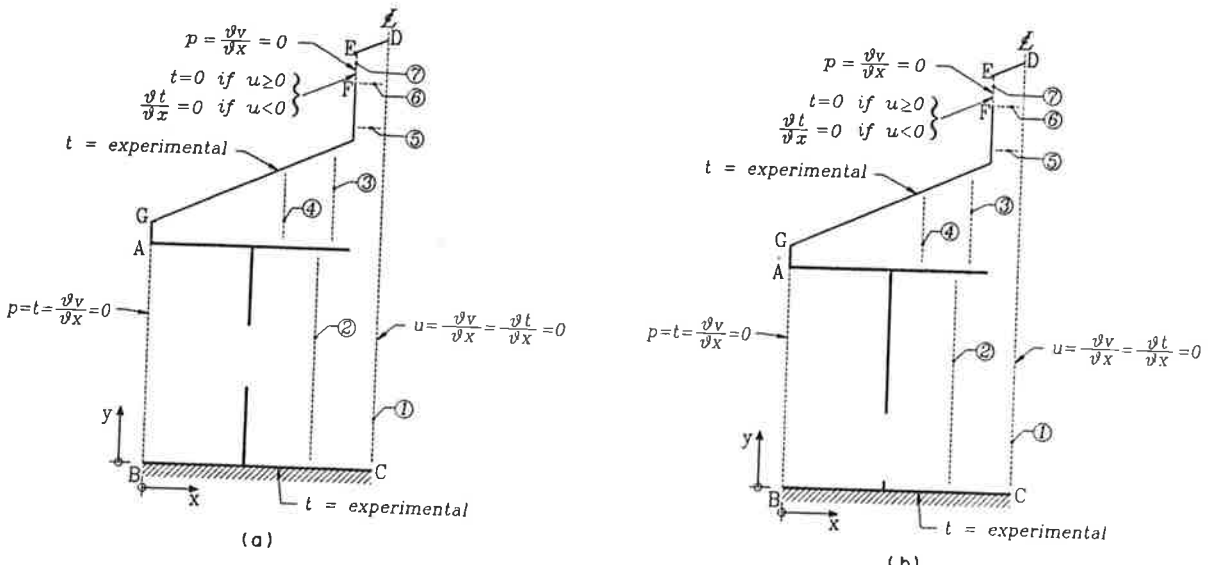

Fig. 5. Scheme of the section studied: (a) geometry #1; (b) geometry #2.

- At the chimney exit, the pressure recovery due to the buoyant jet is assumed to be negligible.

Numerical method

A complete description of the numerical technique is reported elsewhere [28], and only the main features of the method will be summarized.

The numerical method used to solve equations (1)–(4), with boundary conditions (5)–(7), is based on a *Finite Volume* segregated procedure. The solution domain is subdivided into small subdomains—*finite volumes* or *control volumes*—by a variable size rectangular grid. A staggered grid is used, on which all scalar quantities are located at the center of the finite volumes, while the velocity components are located at the volume faces. The incline of the roof was simulated by performing local mesh refinement combined with a control-volume *blocking* technique as described in [29]. Numerical tests conducted to assess this procedure indicate adequate accuracy and reliability.

For the general variable ϕ, the discretized conservation equation at a point P is written in the form:

$$a_P\left(1+\frac{1}{E}\right)\phi_P = \sum_{nb} a_{nb}\phi_{nb} + b + \left(\frac{a_P}{E}\right)\phi_P^0 \qquad (8)$$

where the summation extends to the surrounding *nb* finite volumes, and ϕ_P^0 is the value of ϕ_P at the previous iteration cycle. Equation (8) embodies the E-factor formulation suggested in [30], and the convection and diffusion fluxes are approximated by a hybrid scheme [29]. The solution technique is based upon an enhanced SIMPLE-C algorithm [30], accelerated by means of a *Global Mass Correction* procedure [31].

The computation was performed by enclosing the entire domain in a 56×96 non-uniform, Cartesian grid. The choice is based on the results of previous grid convergence tests for laminar and turbulent free convection [32]. Approximately 2000 iterations were required to achieve convergence for each of the two geometries considered.

RESULTS AND DISCUSSION

During the experimental tests, the thermal radiation provided by the solar simulator, produced averaged temperatures in the range 35.5°C to 44.5°C, as measured at 6 different locations on the roof. The *Rayleigh* number for the model, based on ambient *reference* temperature, $T_0 = 23.8$°C, and a maximum roof temperature, $T_1 = 44.5$°C, was estimated at 1.9×10^8. This value, with $Pr = 0.7$, was used in the numerical simulations.

Figures 6 and 7 depict vector plots of the computed velocity field inside the model for the two arrangements.

From these figures, the following observations can be made:

- Hot air exits through the chimney, as it may be expected, causing a drop in internal pressure, and forcing *cooler* air to be drawn in through the window;
- The flow pattern inside the building, below ceiling level, is very sensitive to window geometry: for geometry #1, the incoming air stream moves along a direct path from window to ceiling aperture, while for geometry #2 the air moves almost vertically along the wall to the ceiling, where it turns towards the ceiling aperture;
- Contrary to what one might expect, there is little expansion of the incoming air as it enters the building;
- Air velocities inside the building model are generally very low, suggesting that the desired *cooling* effect

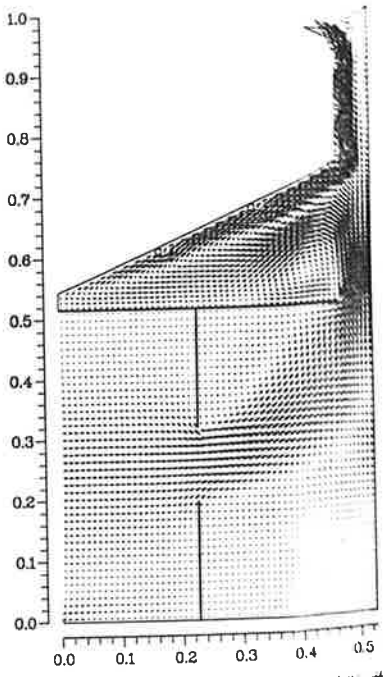

Fig. 6. Velocity vector plot for geometry #1.

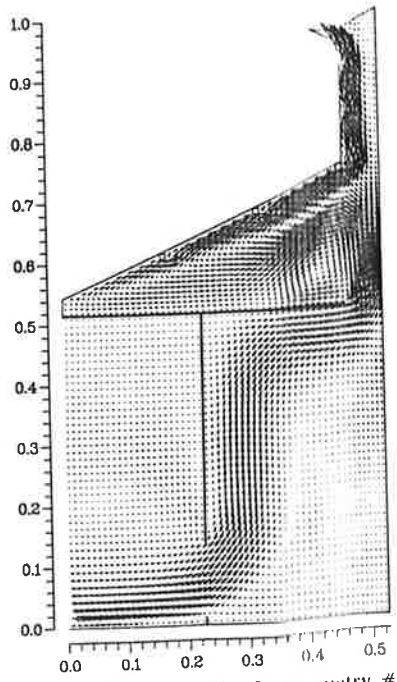

Fig. 7. Velocity vector plot for geometry #2.

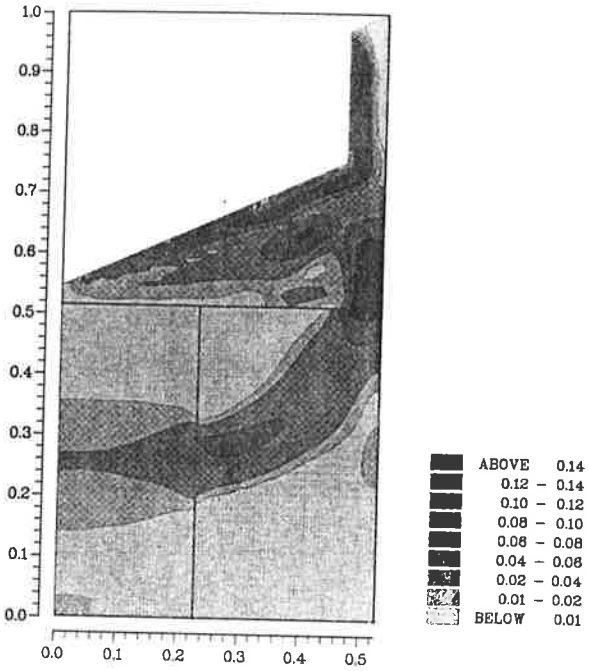

Fig. 8. Velocity magnitude map for geometry #1.

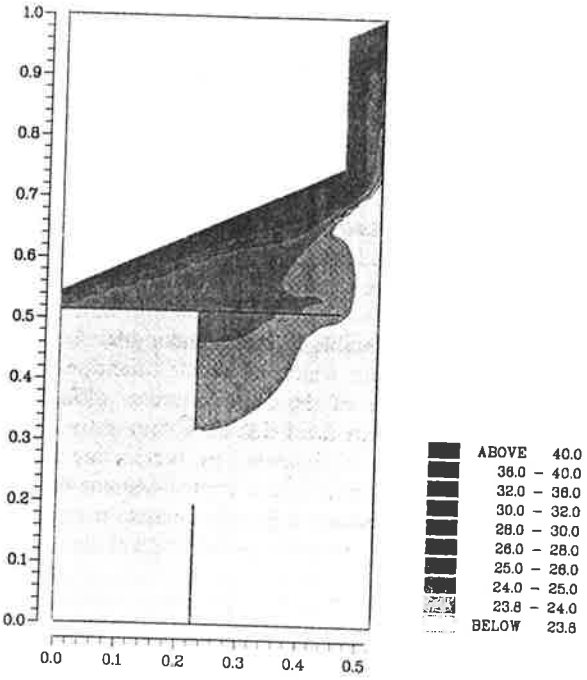

Fig. 10. Temperature map for geometry #1.

may be less than anticipated. This is further illustrated in the shaded plots of dimensional velocity modulus, depicted in Figs 8 and 9;

- The flow field above the ceiling exhibits an almost identical pattern for both geometries;
- Flow visualization confirmed that most of the above characteristics are, indeed, observed in the small-scale model, in particular, the separation bubble in the under-roof region, was clearly identified for both geometries;
- Large flow velocities are computed along the inclined roof surfaces, due to the higher buoyancy forces induced by the large temperature difference.

In Figs 10 and 11, the dimensional temperature maps for geometries #1 and #2 are presented. The temperature increase at ceiling level was computed to be less than 0.1% of the maximum roof temperature, and in this respect, the solar chimney performs better than most traditional roof ventilation systems.

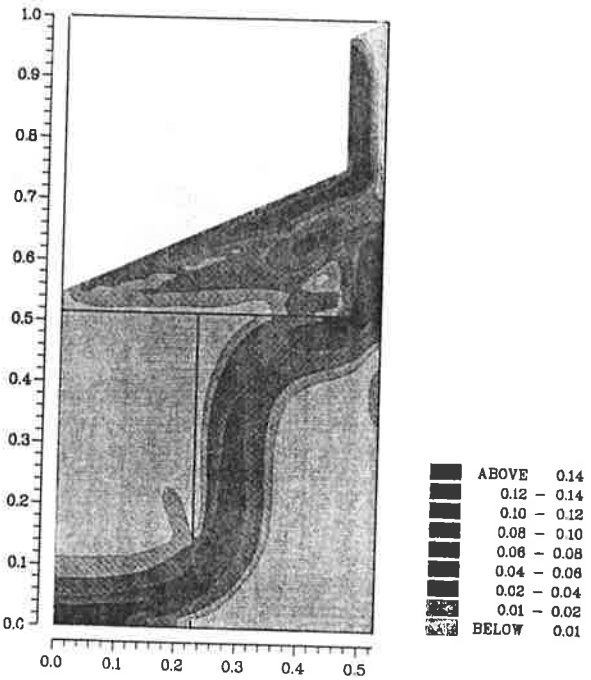

Fig. 9. Velocity magnitude map for geometry #2.

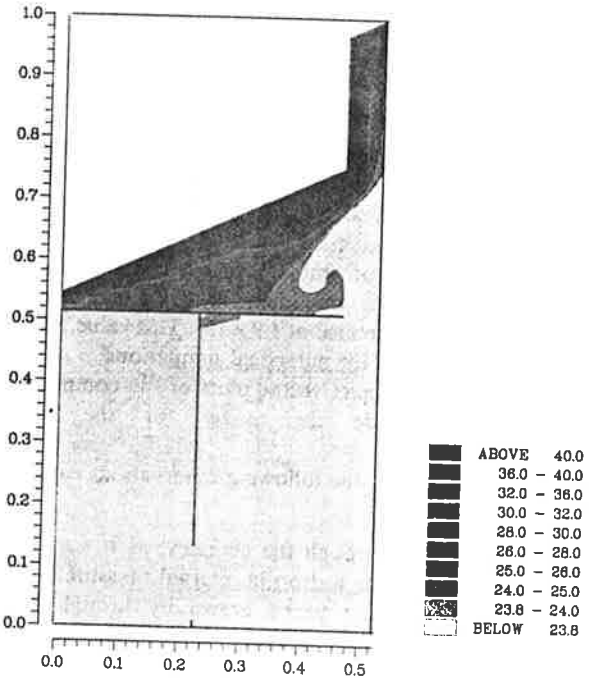

Fig. 11. Temperature map for geometry #2.

In Fig. 12(a) and (b), measured (symbols) *vs* computed (full line) temperatures are compared at section 1 (cf. Fig. 5) for geometries # 1 and # 2 respectively. While the temperature profiles—measured and computed—seem to be unaffected by the window position, it should be noted that the numerical analysis predicts a higher level of thermal stratification, and higher air temperatures at the chimney exit level. The agreement between computations and experimental results is, nevertheless, satisfactory. Computed and measured temperature profiles are reported in Figs 13, 14 and 15 for sections 2, 3 and 4 respectively. For all sections, measurements and computations are consistent in that neither is sensitive to window position. The level of thermal stratification tends to be overpredicted by the numerical model, but the qualitative agreement is considered acceptable for sections 2 and 3. The lower thermal stratification measured at section 4, for both geometries, may be attributed to some turbulence or unsteadiness in the flow field, enhancing air mixing which in turn smears away the vertical temperature gradient.

Figure 16 reports measured and computed temperatures at sections 5 and 6 (cf. Fig. 5) across the chimney, for both geometries. The computed temperatures tend to be higher than the experimental data in the vicinity of the chimney walls, while the experimental values along the centreline are underpredicted. A possible explanation for this discrepancy lies with the choice of a temperature average as the boundary condition at the chimney walls.

Measured and computed air velocities at the chimney exit, Section 7, are finally given in Fig. 17. Although the time-averaged velocity measurements have, at best, an estimated accuracy of $\pm 20\%$, the comparison between measured and computed results is still worthwhile, since velocity magnitudes, and profiles, are in reasonable agreement.

CONCLUDING REMARKS

From the experimental and numerical results, the following conclusions can be made:

- The concept of using a solar chimney, to induce an air flow within the building, seems to work. However, the *cooling* effect appears to be weakest

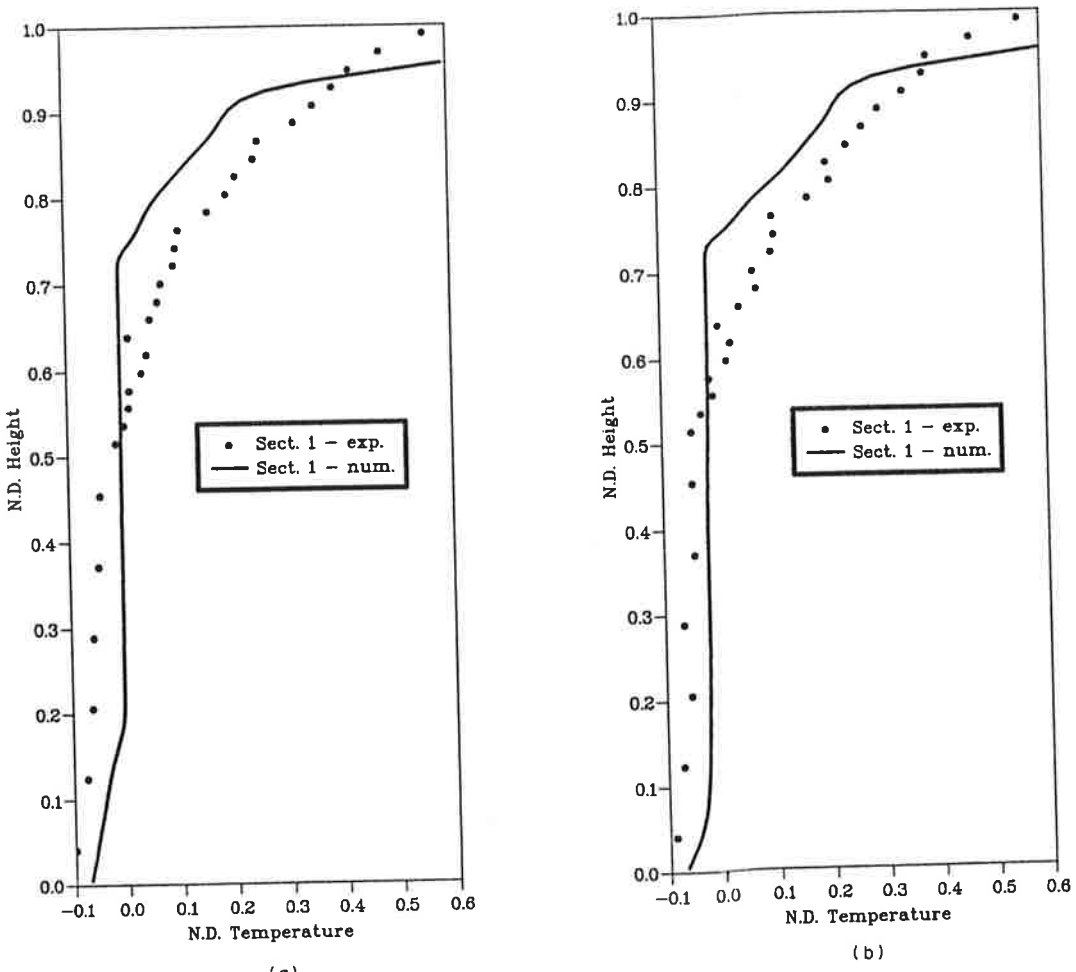

Fig. 12. Temperature profiles at section 1: (a) geometry # 1; (b) geometry # 2.

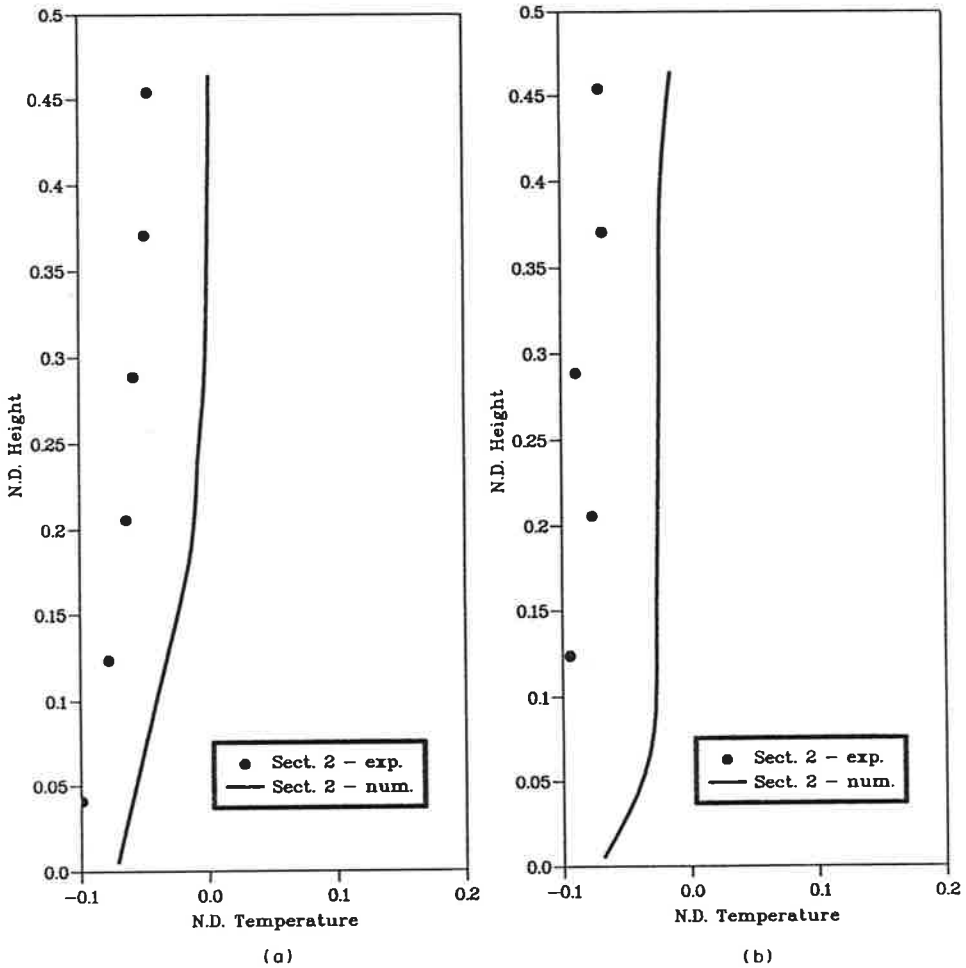

Fig. 13. Temperature profiles at section 2: (a) geometry #1; (b) geometry #2.

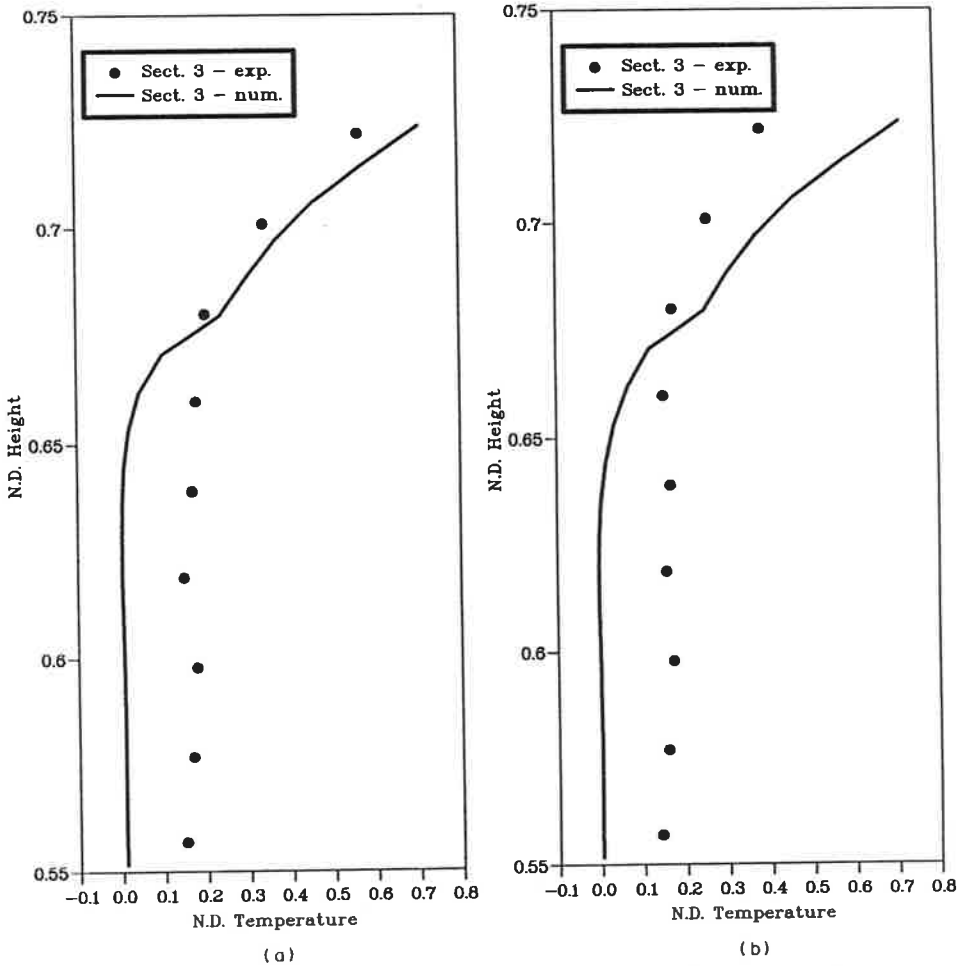

Fig. 14. Temperature profiles at section 3: (a) geometry #1; (b) geometry #2.

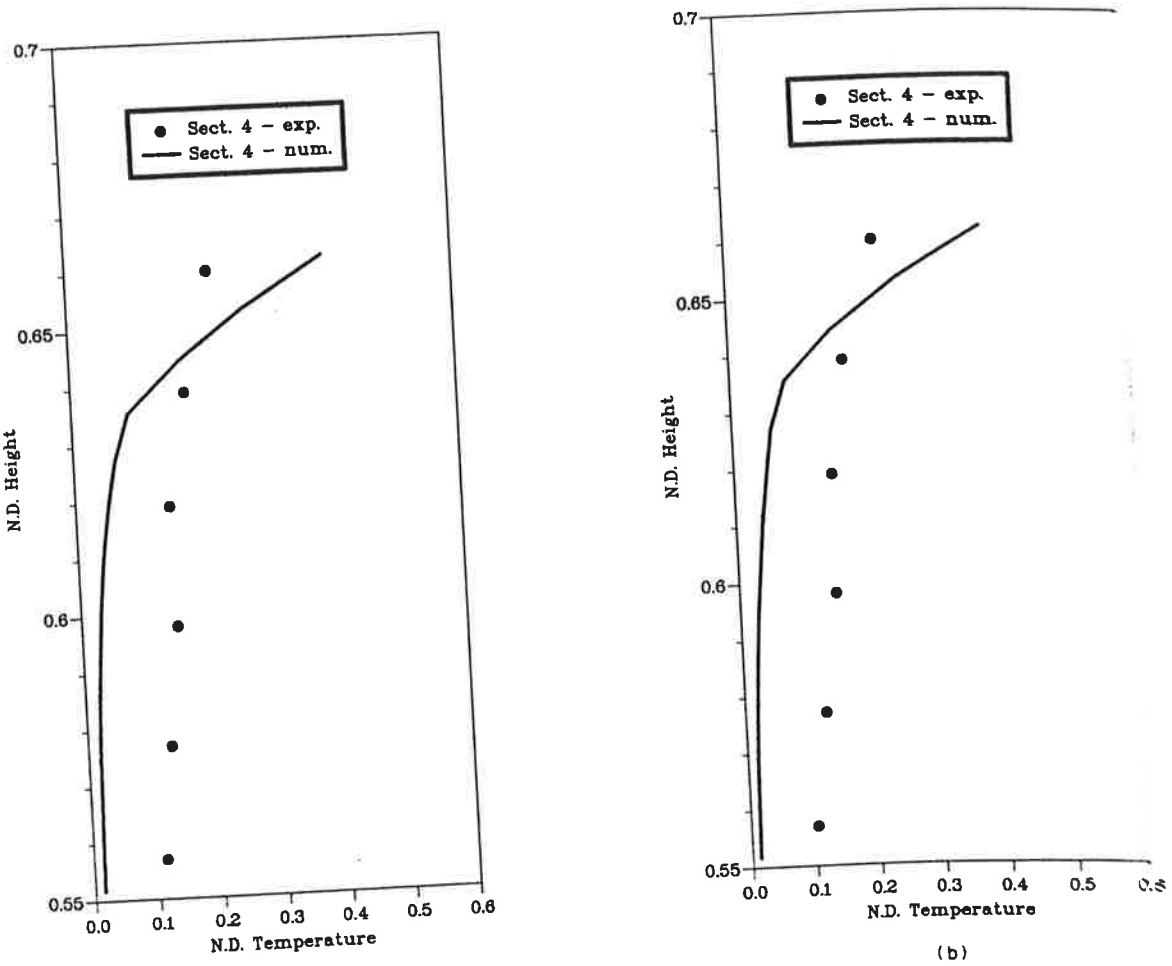

Fig. 15. Temperature profiles at section 4: (a) geometry #1; (b) geometry #2.

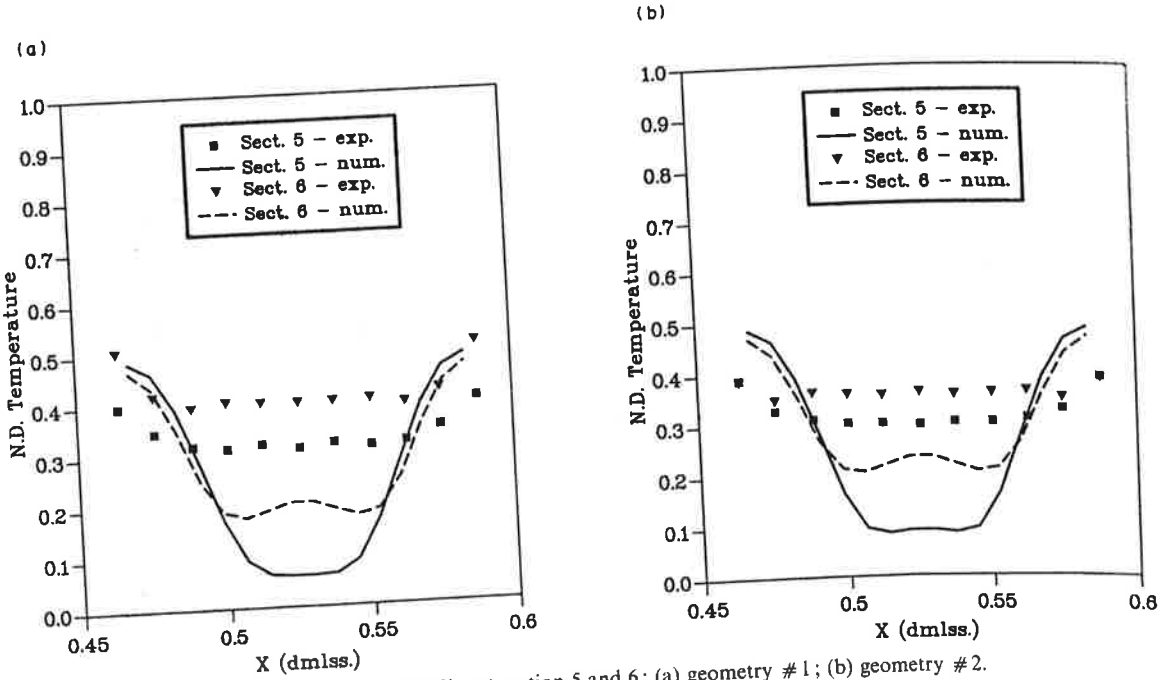

Fig. 16. Temperature profiles at section 5 and 6: (a) geometry #1; (b) geometry #2.

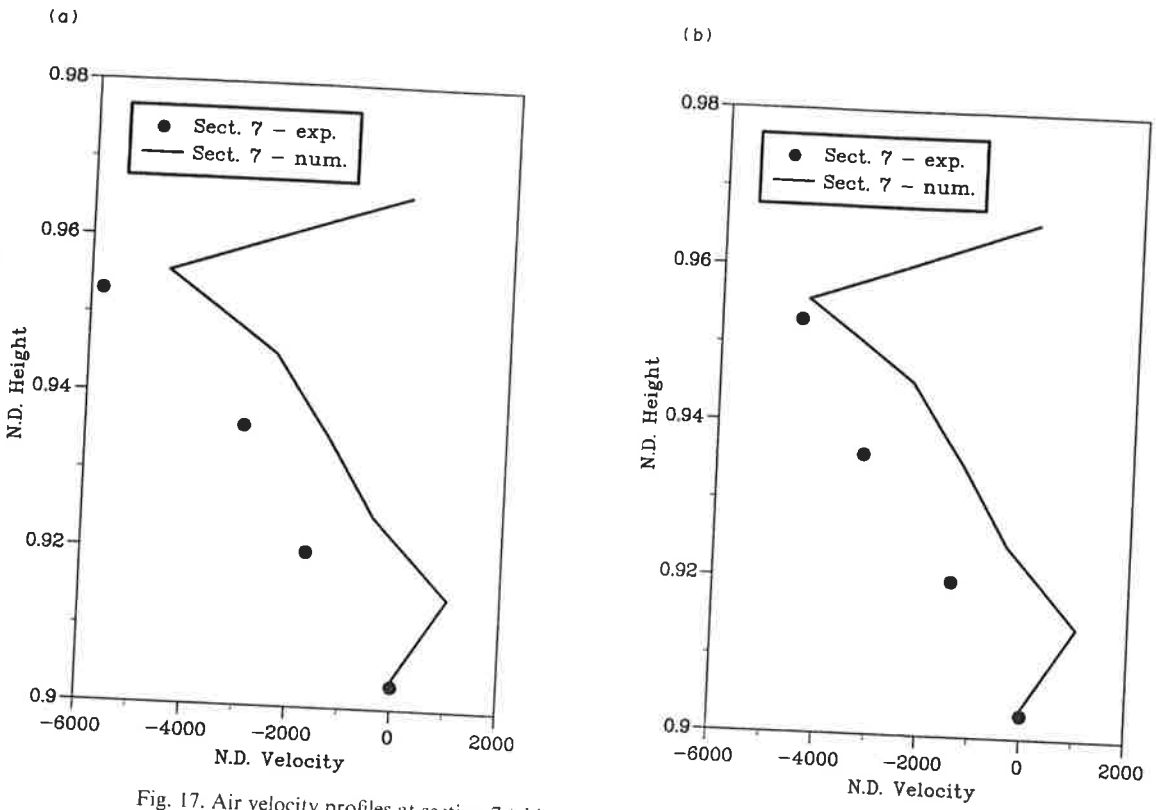

Fig. 17. Air velocity profiles at section 7 (chimney exit): (a) geometry #1; (b) geometry #2.

where it is most needed—i.e. in the living space. Alternative solar chimney and window designs may be expected to improve the situation.

- The predicted flow pattern is in good agreement with the experimental flow visualization.
- The quantitative agreement between experimental and numerical results is encouraging. Major causes of discrepancy may be attributed to the boundary conditions, and eventually the presence of turbulence or unsteadiness in the flow inside the experimental model, and three-dimensional effects, which were not accounted for in the simulations.

Finally, it should be noted that the data obtained in small-scale models may prove to be of critical importance in the development and testing of advanced computer simulation programs.

Acknowledgements—The ICTP* Italian Labs Program, coordinated by Prof. G. Furlan, supported one of the authors (M. Imbabi), while on sabbatical leave at Università di Trieste. The computational work was performed at the Centro di Calcolo dell'Università di Trieste. Thanks are also due to the technical staff (E. Bossi, F. Clarich and W. Moze) for assisting in the experimental tests. The present work was partially funded by the Consiglio Nazionale delle Ricerche, Italy (CNR Grant No. 89.04965.07) and Ministero Pubblica Istruzione—Fondi 40%.

REFERENCES

1. V. Olgyay, *Design with Climate*, Princeton University Press (1963).
2. E. Arens, L. Zeren, R. Gonzalez, L. Berglund and P. E. McNall, A New Bioclimatic Chart for Environmental Design, *Proc. Int. Building Energy Management Congress*, Portugal, 645–657 (1980).
3. E. W. Hamilton (ed), Space Heating with Solar Energy, *Proc. of a course—symposium at M.I.T.*, Publ. by Albert Farwell Bemis Foundation, M.I.T. (1954).
4. A. Goetzberger and W. Stahl, Self-sufficient Solar House 2000, *Proc. 2nd Int. Workshop TIM for Passive Solar Applications*, Freiburg (1988).
5. R. Costa, P. Riva, O. Barduzzi, I. Golubovic' and M. Diaz, Architettura Bioclimatica nell' Area Caldo-umida dei Territori Yoruba (Nigeria), *Energia e Ambiente Costruito—Tradizione e Innovazione*, Udine (1986).
6. B. Givoni, Options and Applications of Passive Cooling, *Energy and Buildings*, **7**, 297–300 (1950).
7. K. I. Parczewski and P. N. Renzi, Scale Model Studies of Temperature Distributions in Internally Heated Enclosures, *ASHRAE Journal*, **5**, 60–68 (1963).
8. W. Moog, Room Flow Tests in a Reduced Scale, *ASHRAE Transactions*, **87**, 1162–1181 (1981).
9. E. B. Maldonado, G. H. Junkhan and J. E. Woods, Use of a Gas Mixture for Experimental Modelling

* International Centre for Theoretical Physics, Trieste, Italy.

of Mixed Free and Forced Convection in Enclosures, *Proc. 7th Int. Heat Transfer Conf.*, Munich, **3**, 453–458 (1982).
10. D. D. Weber, W. O. Wray and R. J. Kearney, Similitude Modelling of Interzone Heat Transfer by Natural Convection, *Proc. 4th Nat. Passive Solar Conference*, Kansas City, 231–234 (1979).
11. N. Nakahara, T. Goto, Y. Miyagawa, M. Kobayashi, T. Yasuda and S. Ito, Verification of Similarity Theory on Space Air Distribution and Study on Occupied Zone Air-conditioning for Large Spaces through Scaled Model Experiments and Actual Measurements, *ASHRAE Int. Best Paper*, New York (1975).
12. M. S. Imbabi, Control Systems in Buildings, M.Sc. Dissertation, Brunel University, U.K. (1980).
13. M. S. Imbabi, Computer Validation of Scale Model Tests for Building Energy Simulation, *Int. J. of Energy Research*, **14**, 727–736 (1990).
14. T. J. Wiltshire and A. J. Wright, Advances in Building Energy Simulation in the U.K.—The Science and Engineering Research Council's Programme, *Energy and Buildings*, **10**, 175–183 (1990).
15. P. V. Nielsen, A. Restivo and J. H. Whitelaw, Buoyancy-affected Flows in Ventilated Rooms, *Num. Heat Transfer*, **2**, 115–127 (1979).
16. P. V. Nielsen, Moisture Transfer in Air Conditioned Rooms and Cold Stores, Paper No. 1.2.1, Procs. 2nd Int. CIB/RILEM Symposium on *Moisture Problems in Buildings*, Rotterdam (1974).
17. G. E. Whittle, Computation of Air Movement and Convective Heat Transfer Within Buildings, *Int. J. of Ambient Energy*, 7, 151–164 (1986).
18. H. B. Awbi, Application of Computational Fluid Dynamics in Room Ventilation, *Bldg Envir.* **24**, 73–84 (1989).
19. S. Murakami and S. Kato, Numerical and Experimental Study on Room Airflow—3-D Predictions using the k–ε Turbulence Model, *Bldg Envir.* **24**, 85–97 (1989).
20. Q. Chen, J. van der Kool and A. Meyers, Measurements and Computations of Ventilation Efficiency and Temperature Efficiency in a Ventilated Room, *Energy and Buildings*, **12**, 85–99 (1988).
21. Q. Chen, Comfort and Energy Consumption Analysis in Buildings with Radiant Panels, *Energy and Buildings*, **14**, 287–297 (1990).
22. N. C. Markatos, M. R. Malin and G. Cox, Mathematical Modelling of Buoyancy-induced Smoke Flow in Enclosures, *Int. J. Heat Mass Transfer*, **25**, 63–75 (1982).
23. M. S. Imbabi, A General Procedure for the Small-Scale Modelling of Buildings, *Int. J. of Energy Research*, **14**, 311–321 (1990).
24. E. Nobile, A. C. M. Sousa and G. S. Barozzi, Accuracy of Two-Equation Turbulence Modelling in Free Convection, Procs. 6° Int. Conf. on *Numerical Methods in Thermal Problems*, Swansea, U.K., Part 1, 600–610 (1989).
25. M. A. Leschziner, Modelling Turbulent Recirculating Flows by Finite-Volume Methods—Current Status and Future Directions, *Int. J. Heat and Fluid Flow*, **10**, 186–200 (1989).
26. R. A. W. M. Henkes, Natural-Convection Boundary Layers, Ph.D. Thesis, Delft University, The Netherlands (1990).
27. W. A. Schreüder, J. P. Du Plessis, Simulation of Air Flow About a Directly Air Cooled Heat Exchanger, *Bldg Envir.* **24**, 23–32 (1989).
28.. E. Nobile, T. Russo and G. S. Barozzi, An Efficient Parallel Algorithm for the Numerical Solution of Navier-Stokes Equations using FORTRAN Structured Multiprogramming, in *Applications of Supercomputers in Engineering: Fluid Flow and Stress Analysis Applications*, Eds. C. A. Brebbia and A. Peters, Southampton, U.K. 3–14 (1989).
29. S. V. Patankar, Numerical Heat Transfer and Fluid Flow, McGraw-Hill, New York (1980).
30. J. P. Van Doormaal and G. D. Raithby, Enhancements of the SIMPLE Method for Predicting Incompressible Fluid Flows, *Num. Heat Transfer*, 7, 147–163 (1984).
31. V. M. Theodossiou, A. C. M. Sousa and L. N. Carlucci, Flow Field Predictions in a Model Heat Exchanger, *Comp. Mech.* **3**, 419–428 (1988).
32. E. Nobile, A. C. M. Sousa and G. S. Barozzi, Turbulent Buoyant Flows in Enclosures, *Proc. 9th Int. Heat Transfer Conf.*, Jerusalem, **2**, 543–548 (1990).